CORE AND SUB-CHANNEL EVALUATION OF A THERMAL SCWR

XIAO-JING LIU* and XU CHENG
School of Nuclear Science and Engineering, Shanghai Jiao Tong University
Dong Chuan Road 800, Shanghai, 200240, China
*Corresponding author. E-mail : xiaojingliu@sjtu.edu.cn

Received November 20, 2008
Accepted for Publication January 11, 2009

A previous study demonstrated that the two-row fuel assembly has much more favorable neutron-physical and thermal-hydraulic behavior than the conventional one-row fuel assemblies. Based on the newly developed two-row fuel assembly, an SCWR core is proposed and analyzed.

The performance of the proposed core is investigated with 3-D coupled neutron-physical and thermal-hydraulic calculations. During the coupling procedure, the thermal-hydraulic behavior is analyzed using a sub-channel analysis code and the neutron-physical performance is computed with a 3-D diffusion code. This paper presents the main results achieved thus far related to the distribution of some neutronic and thermal-hydraulic parameters. It shows that with adjustment of the coolant and moderator mass flow in different assemblies, promising neutron-physical and thermal-hydraulic behavior of the SCWR core is achieved. A sensitivity study of the heat transfer correlation is also performed.

Since the pin power in fuel assemblies can be non-uniform, a sub-channel analysis is necessary in order to investigate the detailed distribution of thermal-hydraulic parameters in the hottest fuel assembly. The sub-channel analysis is performed based on the bundle averaged parameters obtained with the core analysis. With the sub-channel analysis approach, more precise evaluation of the hot channel factor and maximum cladding surface temperature can be achieved. The difference in the results obtained with both the sub-channel analysis and the fuel assembly homogenized method confirms the importance of the sub-channel analysis.

KEYWORDS : Supercritical Water Cooled Reactor (SCWR), Core Design, Coupling Analysis, Sub-channel Analysis

1. INTRODUCTION

The supercritical water cooled reactor (SCWR) operates at high pressure and temperature, and eliminates the coolant boiling phenomenon so that the coolant remains in a single phase throughout the reactor. As a consequence, the thermal efficiency of the SCWR can dramatically increase up to 44%. Based on the outstanding achievement of both the water-cooled reactor and supercritical fossil-fired power plant technology, SCWR can maintain smooth technical continuity [1].

In the past several years, extensive R&D activities covering various aspects of SCWR development have been launched around the world. Several conceptual designs of SCWRs have been proposed in the open literature. Most of these concepts are based on the thermal spectrum. Efforts have also been made to design SCWR reactor cores with a fast neutron spectrum [1].

The thermal spectrum SCWR fuel assemblies (FA) proposed in the open literature can be divided into two classes, i.e. PWR-type and BWR-type. The PWR-type fuel assembly stems from a PWR similar fuel assembly and is of similar size. The fuel pins can be arranged in a square lattice or in a hexagonal lattice [2, 3]. Compared to the PWR-type fuel assembly, the BWR-type fuel assembly is small. The fuel pins can be arranged in either a square or hexagonal lattice. Due to insufficient moderation capability inside the BWR-type fuel assembly, additional water gaps between fuel assemblies are required [4, 5].

The so-called PWR-type square lattice with one row of fuel rods between moderator channels has also been widely used. Analyses [2, 3] revealed that in this one-row fuel assembly structure, a large neutronic hot spot factor, and subsequently a large hot-channel factor, occurs. For the BWR-type fuel assemblies proposed in the open literature, large water gaps between the fuel assemblies will lower the power density sharply [4, 5]. More recently, fuel assemblies of a PWR-type square lattice with two row fuel rods between the moderator channels (referred to as a two-row fuel assembly) have been proposed [6].

A recent study showed that the two-row fuel assembly has much more favorable neutron-physical and thermal-hydraulic behavior than the conventional one-row fuel assemblies [6].

At the same time, the counter-current flow mode with moderator and coolant flowing in the opposite directions is widely applied to provide good moderation in the upper part of the core [1]. Recently, intensive investigations have been carried out to reduce the non-uniformity of fluid temperature and to mitigate the hot-channel factor. One of the most widely applied approaches is to utilize multi-flow path concepts [2, 4]. However, this introduces some additional challenging issues in complex core structures and decay heat removal at loss of pump head transients.

This paper proposes a thermal spectrum SCWR core design using a two-row fuel assembly. Some of the main findings of the coupling results related to this SCWR design are summarized. A sensitivity study of the heat transfer coefficient for both coolant and moderator channels is carried out. Under consideration of the main results achieved thus far, a recommendation for the design of thermal SCWR cores is given.

Investigations are also carried out to perform sub-channel analysis, wherein the cladding temperature is accurately calculated and it is precisely determined whether the cladding temperature can be kept below the design limit. Recently, Cheng et al. [7] carried out a sub-channel calculation using the STAFAS code to obtain a detailed distribution of various parameters in an SCWR fuel assembly. Their work, however, focuses only on the thermal hydraulic performance. Waata et al. [8] developed a coupled simulation approach with MCNP and the sub-channel code STAFAS for a fuel assembly analysis. Although this gives detailed local characteristics of the fuel rods and sub-channels, application of the coupling procedure is restricted to one fuel assembly and requires extremely large computational efforts. The non-uniformity of the power and mass flow rate distribution over the reactor core is beyond consideration. This would lead to an underestimation of power generation in the hottest fuel assembly. Yamaji et al. [9] performed a pin-wise power reconstruction within fuel assemblies. Based on the pin-wise power distribution, sub-channel calculation is performed to obtain the detailed coolant and cladding temperature of the sub-channels and the fuel rods. This approach requires a large amount of neutronic calculations to derive an accurate pin-wise power distribution in the assembly. Liu and Cheng [10] evaluated the cladding peak temperature by a 3-D core coupling calculation. In the first step, each fuel assembly is homogenized for the coupled core analysis of neutronics and thermal hydraulics. Based on the fuel assembly averaged parameters, several fuel assemblies with critical parameters, e.g. highest coolant temperature, are selected for further detailed investigations.

In the second step, a coupled analysis of thermal-hydraulics in the sub-channel scale and neutron-physics in the pin-wise scale is then carried out for the selected critical fuel assemblies, in order to determine parameter distribution inside the fuel assembly. The fuel assembly averaged values, such as fuel assembly power, mass flux, and moderator flow rate, are taken from the coupling core calculation.

2. ASSEMBLY PARAMETER

In a previous study [6], the two-row fuel assembly shows better thermal-hydraulic and neutronic performance than the conventional one-row assembly. Based on the two-row assembly concept, a new SCWR core design is proposed. The two-row assembly is illustrated in Fig. 1 and the design parameters are presented in Table 1. Some neutronic parameters of the two-row assembly are summarized in Table 2. The data indicate that all the temperature reactivity coefficients are kept negative.

3. CORE DESIGN PARAMETERS

Fig. 2 shows the vertical cross-section and the flow scheme of the reactor pressure vessel (RPV). When entering the RPV, the feed water is divided into two parts. One part flows through the down-comer to the lower plenum, whereas the other part goes upwards to the upper plenum of the pressure vessel. From there it enters the moderator channels and then exits the moderator channels in the lower plenum, where it mixes with the first part of the feed water. The total water then flows through the fuel

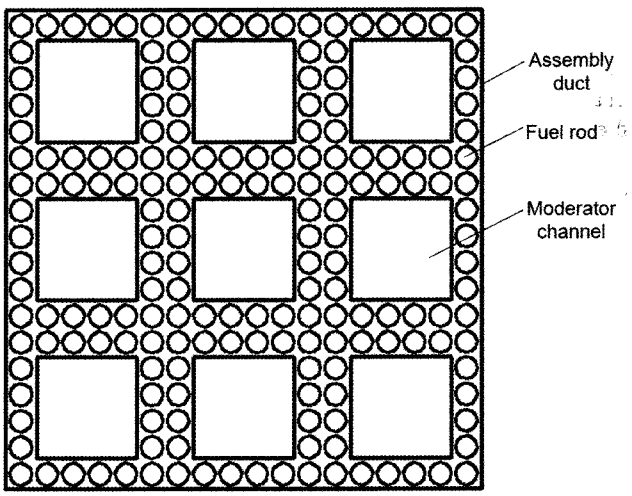

Fig. 1. Sketch of Two-row Fuel Assembly [6]

Table 1. Parameters of Two-row Assembly [6]

Fuel pin lattice	Square 18 × 18 array
Number of fuel rods per assembly	180
Number of moderator tube per assembly	9
Diameter of the fuel rod (mm)	8.0
Diameter of the fuel pin (mm)	6.84
Cladding thickness (mm)	0.5
Assembly wall thickness (mm)	2.0
P/d (-)	1.2
Duct wall clearance (mm)	1.0
Moderator channel wall clearance (mm)	1.0
Assembly side (mm)	177.2
Moderator tube inner/outer side length (mm)	38.0/37.0
Volume ratio (moderator/fuel) (-)	3.06

Table 2. Neutronic Parameters of the Assembly

Results \ Fuel enrichment (wt %)	2.5	3.5	4.0	5.0	6.5
K_∞	0.938	1.060	1.106	1.178	1.255
Fuel Doppler temperature reactivity coefficient (10^{-5}/K)	-1.71	-1.74	-1.78	-1.69	-1.73
Moderator temperature reactivity coefficient (10^{-5}/K)	-80.57	-90.25	-93.47	-97.19	-100.88
Coolant temperature reactivity coefficient (10^{-5}/K)	-24.70	-26.88	-27.38	-27.93	-27.85

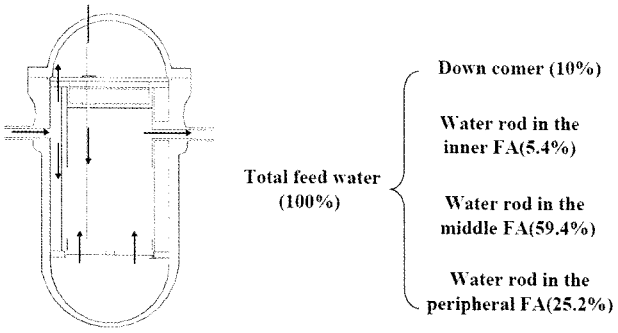

Fig. 2. Counter-current Flow of the Thermal SCWR Core and the Feed Water Flow Distribution

channels and removes the heat generated in the fuel rod pins. With this design the water temperature at the pressure vessel exit is the same as the average temperature at the exit of the cooling channels.

The design parameters of the core are summarized in Table 3. The gap width between fuel assemblies is from the current PWR design [11]. Considering the non-homogeneities effects of the assembly and the refuel process, a large gap should be considered in future work.

The feed fuel enrichment must be high enough to provide the reactivity needed for the fuel cycle length. Fuel assemblies of 3 different enrichments are used. The initial fuel enrichment varied between 4.0% and 6.5%, as shown in Fig. 3. Burn-up optimization studies still need to be done.

The core contains 249 fissile fuel assemblies in the inner zone and 52 reflector assemblies in the peripheral area. The lowest enrichment assemblies are arranged in the central portion of the core while the high enrichment assemblies are placed in the peripheral area. Since the highly enriched fuel is placed in the region with the highest neutron leakage, the assembly power peak can be reduced. The reactor core is surrounded by a "reflecting" material (water with a density of 0.8g/cm^3) to reduce the ratio of peak flux to the flux at the edge of the core fuel area. Flattening of the neutron flux can thereby be achieved. Fig. 4 shows the identification numbers of the assemblies in the 1/4 core.

Table 3. Design Parameters of the Proposed SCWR Core

Core pressure(MPa)	25.0
Core thermal/electrical power (MW)	3576.64/1573.72
Average linear power density (kW/m)	19.0
Coolant inlet outlet (°C)	280.0/508.0
Thermal efficiency (%)	44.0
Number of fissile assembly in core/ reflector	249/52
Core flow rate (kg/s)	1820.0
Assembly fuel enrichment (wt %)	4.0/ 5.0/ 6.5
Average core enrichment (wt %)	5.46
Moderator mass flow fraction (%)	90
Active height/equivalent diameter (m)	4.20/ 3.38
MLHGR/ALHGR* (kW/m)	38.9/19.0
Average power density (MW/m^3)	107.7
Material of cladding and water rod, assembly wall	Alloy 718
Average mass flux of the assemblies ($kg/s/m^2$)	903.14
The gap between assemblies (mm)	2.0

*ALHGR: average linear heat generation rate

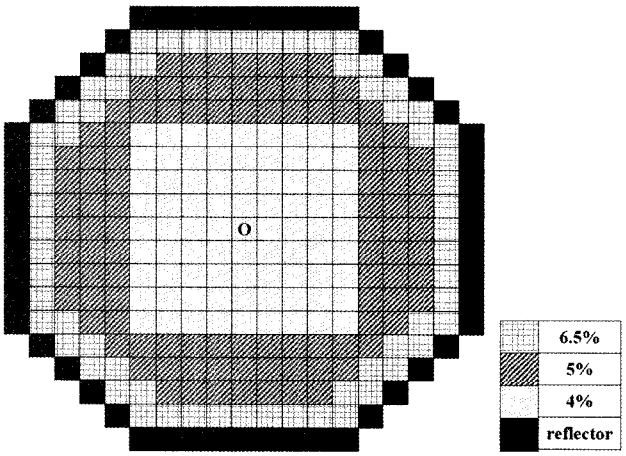

Fig. 3. Fuel Enrichment Distribution

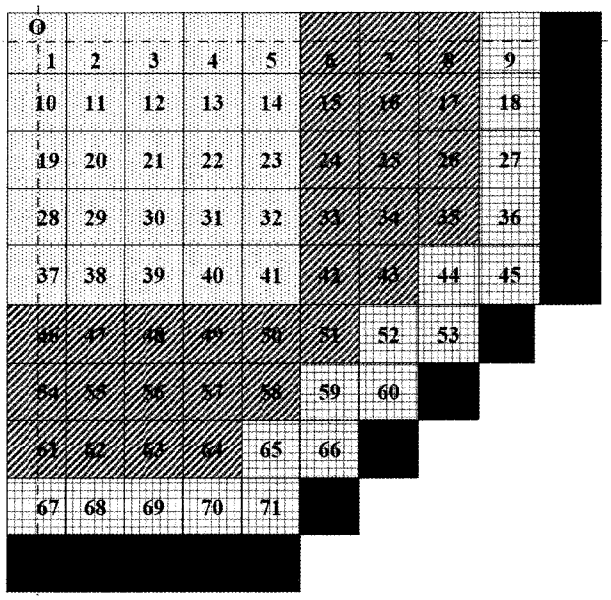

Fig. 4. Identification Number of Assemblies in1/4 Core

4. COUPLING ANALYSIS METHOD

The thermal hydraulic calculation is carried out for a given core power distribution obtained by the neutron-kinetics code SKETCH-N. The sub-channel analysis code COBRA-IV computes the flow and enthalpy distribution in the closed fuel assemblies. To make the COBRA-IV code applicable to SCWR conditions, the thermal-physical properties of supercritical water and a new model for the moderator channel are implemented into the COBRA-IV code. The core is axially divided into 21 nodes. For the thermal-hydraulic calculation, one assembly is treated as

Table 4. Valid Parameter Range of Heat Transfer Correlations [12,13]

Correlation	Pressure (MPa)	Bulk or wall temperature(°C)	Mass flux (kg/m^2/s)	Heat flux (kW/m^2)	Flow geometry
Swenson	22.7-41.3	T_b=70-575 T_w= 93-649	542-2150	200-1800	D =9.4mm upward flow
Bishop	22.6-27.5	T_b=294-525	680-3600	310-3500	D=2.5-5.1mm L/D=30-565
Yamagata	22.6-29.4	T_b =230-540	310-1830	116-930	D=7.5, 10.0mm vertical(downward and upward flow), horizontal
Watts	25	T_b =150-310 T_w= 260-520	160-1060	175-440	D=25~32.2mm upward downward flow
Dittus-Boelter	Sub-critical	-	-	-	10^4<Re <1.2×10^5 0.7<Pr<120
Fuel channel	25	T_b=350-580	350-1250	40-1165	D =4.9mm upward flow
Moderator channel	25	T_b =280-380	350-650	-	D=36.2mm downward flow

one calculation node. The average equivalent diameter of the coolant flow channels is taken for the fuel channel analysis.

From a thermal hydraulic point of view, numerous heat transfer correlations are developed under the supercritical pressure condition [12]. Various heat transfer correlations have been applied to evaluate the heat transfer between the cladding and coolant. However, few analyses of the correlation effect on the moderator heat transfer have been reported in the open literature. The heat transfer correlation will introduce large uncertainties for the axial power distribution and other thermal hydraulic parameters.

Table 4 summarizes the valid parameter range of the selected heat transfer correlations as well as the hydrodynamic conditions of the fuel channel and the moderator channel. According to hydrodynamic conditions, the heat transfer correlations of Bishop [12] Watts [13] are selected as references for flows in fuel channels and in moderator channels, respectively. In addition, several other heat transfer correlations are also applied to evaluate the effect of heat transfer correlations on the cladding temperature and on heat transfer between the moderator channels and fuel channels. Due to the closed assembly design and the water gap between the assemblies, the adjacent fuel assemblies are assumed to be adiabatic.

The neutron-kinetics calculation is carried out for a given distribution of the coolant density, the moderator density, and the fuel temperature. The neutronic model discussed in this paper uses two neutron energy groups

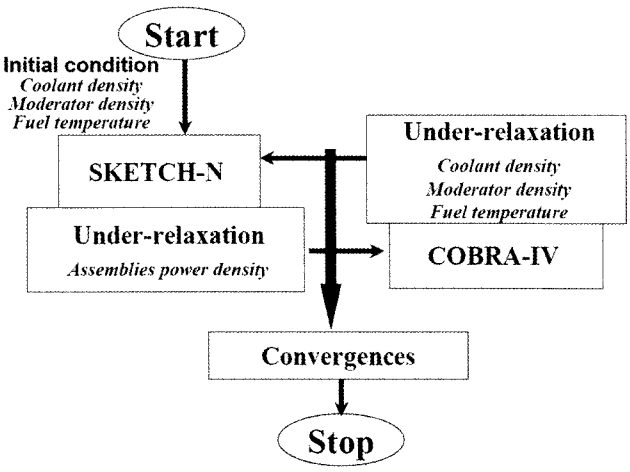

Fig. 5. Flow Chart of the Coupling Procedure

that are divided by 0.625eV. The macroscopic cross-sections are given as polynomial functions of the water density and effective fuel temperature. The macroscopic cross-section is calculated by MCNP based on 69 energy groups.

Fig. 5 schematically illustrates the coupling procedure. The two codes are treated as separate processes and their coupling is realized by the data exchange module between

them. The iterative procedure is repeated until convergence of both the neutron-physical and thermal-hydraulic calculation is attained. An under-relaxation factor (0.3~0.6) is used in this coupling procedure, and a reasonable convergence speed is achieved [6]. For the thermal-hydraulic calculation, one assembly is treated as one calculation node, while for the neutronic analysis one assembly is divided into 4 radial sectors. Therefore, for the coupled calculation, a mapping between the neutronic nodes and thermal-hydraulic nodes is established.

5. ASSESSMENT OF THE CORE PERFORMANCE

With the coupling approach discussed in the previous chapter, the performance of the proposed reactor core is assessed. It is assumed that the coolant flow rate in each fuel assembly can be adjusted by introducing inlet orifices. Fig. 6 shows the coolant flow rate distribution in the 1/4 core. The numbers present the relative coolant flow rate in each assembly. The coolant flow is assigned to match the power of each assembly to obtain a relatively uniform coolant outlet temperature [2].

For the steady state analysis, the moderator inlet and coolant outlet temperature are fixed. The inlet coolant temperature of the fuel assemblies can be varied by controlling the fraction of the moderator flow within the feed water into RPV. Generally, higher core inlet temperature causes accordingly reduced moderation in the lower part of the core. A previous study [6] showed that the axial power peak is in the lower part of the core. To meet the design criteria of the maximum linear heat generation rate (MLHGR, 39kW/m for the steady state) [3], a large moderator flow fraction (e.g. 90%) is needed to flatten the power peak in the lower part of the core. Because the two-row assembly has a large water rod, the moderator temperature is far below the pseudo-critical point. It is not necessary to apply additional materials in the water rod for thermal insulation. On the contrary, enhancement of heat transfer between the fuel channel and the moderator channel can reduce the power peak in the lower part of the core due to feedback of the moderator density.

The mass flow of the moderator is distributed in 3

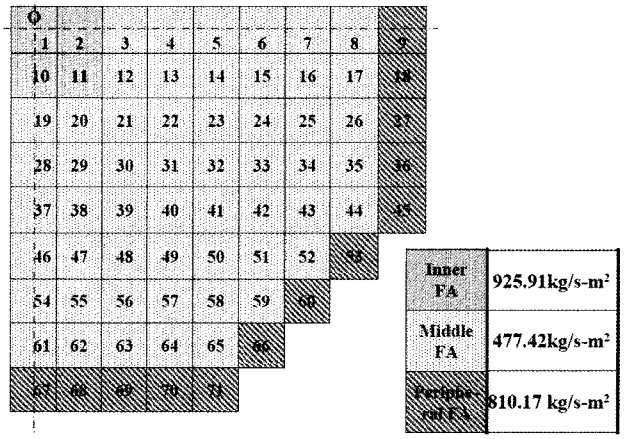

Fig. 7. The Moderator Mass Flux Distribution

0.63	0.651	0.724	0.859	1.064	1.344	1.339	1.112	0.724
0.651	0.673	0.743	0.873	1.071	1.345	1.332	1.103	0.716
0.724	0.743	0.804	0.916	1.093	1.343	1.310	1.072	0.689
0.859	0.873	0.916	0.997	1.129	1.333	1.264	1.003	0.623
1.064	1.071	1.093	1.129	1.174	1.299	1.159	0.949	0.438
1.344	1.345	1.343	1.333	1.299	1.189	1.052	0.565	
1.339	1.332	1.310	1.264	1.159	1.052	0.594		
1.112	1.103	1.072	1.003	0.949	0.565			
0.724	0.716	0.689	0.623	0.438				

Fig. 6. Coolant Flow Rate Distribution (1/4 Symmetric Core)

0.762	0.774	0.779	0.872	1.027	1.308	1.320	1.124	0.781
0.774	0.786	0.792	0.882	1.031	1.306	1.312	1.114	0.772
0.779	0.792	0.831	0.912	1.044	1.299	1.288	1.081	0.742
0.872	0.882	0.912	0.971	1.068	1.284	1.238	1.009	0.672
1.027	1.031	1.044	1.068	1.107	1.251	1.136	0.957	0.475
1.308	1.306	1.299	1.284	1.251	1.155	1.043	0.597	
1.320	1.312	1.288	1.238	1.136	1.043	0.622		
1.124	1.114	1.081	1.009	0.957	0.597			
0.781	0.772	0.742	0.672	0.475				

Fig. 8. Radial Power Distribution in the Reactor Core

different zones, as illustrated in Fig.2. In the present core design, the inner FAs and the peripheral FAs have a larger moderator mass flux, as shown in Fig. 7. The power in these FAs is increased and the radial power distribution is flattened. The power density of each assembly depends on the moderator mass flow and the coolant mass flow in each assembly. The radial and axial power distribution can be changed by changing these values.

With the coolant and moderator mass flow distribution mentioned above, the radial power and axial power distribution are presented in Fig. 8 and Fig. 9, respectively. The radial power peak occurs in FA7 with a value of 1.320. The axial power peak locates in the lower part of the core. It should be pointed out that from the perspective of heat transfer, a large power peak near the core outlet should be avoided due to small specific enthalpy and low heat transfer coefficient at high coolant temperatures. A power peak in the upper part of the core could lead to a sharp increase in the cladding temperature, which should be avoided from the point of view of reactor safety.

The coolant outlet temperature and maximum cladding surface temperature of each assembly are illustrated in Fig. 10. It is of interest that the channel with the largest coolant enthalpy rise locates in FA7 and FA54, while the maximum cladding temperature occurs in FA3 and FA19. The different locations for the maximum coolant temperature and the maximum cladding temperature are due to the complex dependence of the cladding temperature on the coolant enthalpy, FA power, coolant and moderator mass flux, and heat transfer between the coolant and fuel rod.

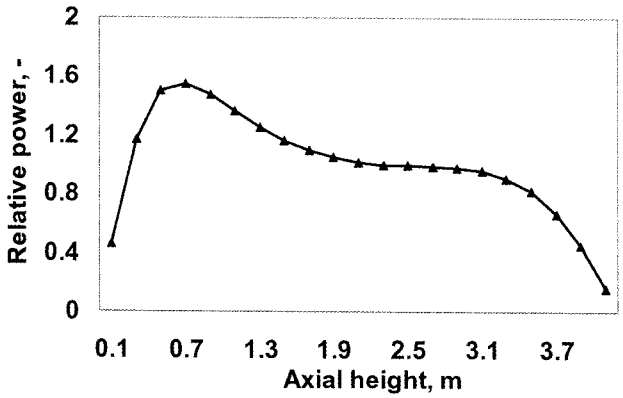

Fig. 9. Axial Power Distribution

471.5 639.1	469.9 631.2	518.7 654.4	511.0 631.3	508.0 615.4	533.0 641.2	539.1 650.2	534.5 650.3	459.8 587.7
469.9 631.2	468.3 624.0	517.1 650.0	510.2 629.2	507.3 614.2	532.2 640.1	538.4 649.4	533.3 649.1	458.1 585.7
518.7 654.4	517.1 650.0	512.0 637.0	508.2 623.5	505.7 611.0	530.0 637.1	535.5 646.1	529.5 645.0	452.1 578.5
511.0 631.3	510.2 629.2	508.2 623.5	506.2 616.1	504.1 607.3	527.0 633.5	530.7 640.9	521.2 636.5	437.9 560.6
508.0 615.4	507.3 614.2	505.7 611.0	504.1 607.3	505.5 607.5	524.6 631.3	522.6 632.9	516.3 631.9	398.4 497.0
533.0 641.2	532.2 640.1	530.0 637.1	527.0 633.5	524.6 631.3	520.6 629.1	519.1 631.4	419.2 529.2	
539.1 650.2	538.4 649.4	535.5 646.1	530.7 640.9	522.6 632.9	519.1 631.4	423.1 533.3		
534.5 650.3	533.3 649.1	529.5 645.0	521.2 636.5	516.3 631.9	419.2 529.2			
459.8 587.7	458.1 585.7	452.1 578.5	437.9 560.6	398.4 497.0				

coolant
cladding

Fig. 10. Outlet Coolant and Maximum Cladding Temperature in each FA

6. SENSITIVE STUDY

6.1 Effect of Heat Transfer Correlation on Maximum Cladding Surface Temperature (MCST)

For the present analysis, the correlations of Bishop [12] and of Watts [13] are selected as references for heat transfer in the fuel channel and water rod, respectively. To identify the effect of heat transfer correlations on the coupling results, several other correlations are applied to the coupling procedure.

Fig. 11 shows the differences between various correlations for given conditions. All the correlations show a heat transfer peak when the fluid bulk temperature is

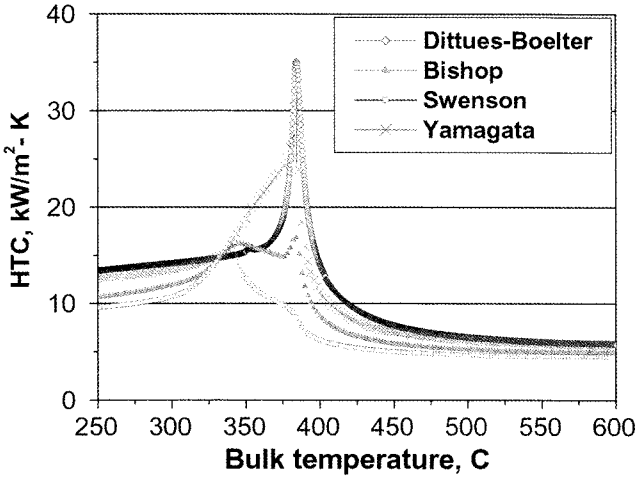

Fig. 11. Heat Transfer Coefficient (HTC) by Different Correlations (P=25MPa, G=1.0 × 10^3kg/s·m^2, Q=1.0 × 10^3kW/m^2, D=0.0049m)

equal to (or below) the pseudo-critical point. The figure indicates that the Dittus-Boelter correlation gives the highest heat transfer coefficient value, while the Swenson correlation shows the lowest value. For the bulk temperature beyond the pseudo-critical point, satisfactory agreement of the heat transfer coefficient value is obtained between different correlations.

Fig. 12a presents the calculated cladding temperature profile in the hot assembly FA3 using different heat transfer correlations. The results indicate that the Swenson and Bishop correlations give a higher maximum cladding temperature, which locates in the upper part of the active height. The other two correlations give a maximum cladding temperature well below the upper design limit of 650°C, which approaches the outlet of the core. Therefore, correct selection of the heat transfer correlation is of crucial importance in assessing the performance of the reactor core design.

In addition, a cladding temperature peak is also observed in the lower part of the active core using the Swenson and Bishop correlation. This peak corresponds to the axial power peak around this region (see Fig. 9). The power peak (correspondence to the heat flux peak) and the thermal hydraulic condition in this region cause a sharp decrease in the heat transfer coefficient (see Fig. 12b). The high cladding temperature peak shows similar behaviour to so-called heat transfer deterioration (see Fig.12b). There is wide consensus that heat transfer deterioration occurs at low mass flux, high heat flux, and temperature conditions [12]:

$$T_b \leq T_{pc} \leq T_w \quad (1)$$

where T_b is the bulk temperature; T_{pc} is the pseudo-critical point; and T_w is wall temperature, which is the cladding surface temperature in the present case. Therefore, heat transfer deterioration only occurs in the lower part of the core, where the coolant temperature is lower than the pseudo-critical value and a large power peak locates. Findings of a previous study indicated that the power peak in the upper part of the core should be reduced as much as possible for the safety criterion of the cladding temperature. In addition, this paper clearly shows that special attention should also be paid to the power peak in the lower part of the core to maintain the maximum cladding temperature well below the upper design limit.

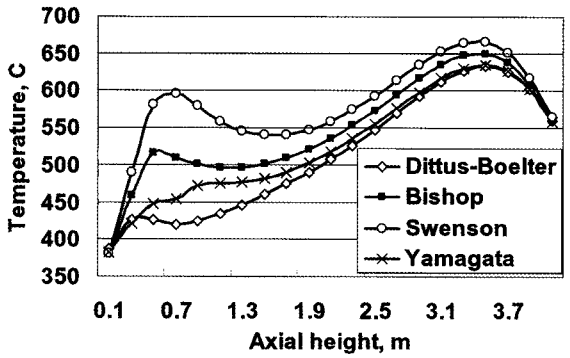

(a) Cladding temperature

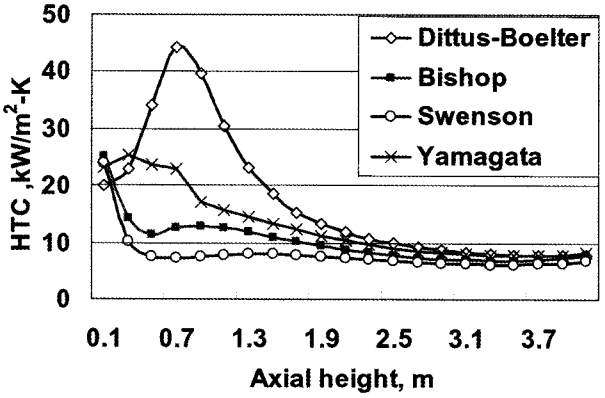

(b) Heat transfer coefficient (HTC)

Fig. 12. Cladding Temperature and HTC Distribution of the Hot Assembly (FA 3)

6.2 Effect of Heat Transfer Correlation for Water Rod

The water rod is hydraulically separated from—but thermally connected to—the fuel channels. Moreover, water in the moderator channels flows in the opposite direction to the fuel channels. The heat transfer between the water rod and fuel channel does not always occur in the same direction. In the upper part of the core, heat is transferred from the fuel channel to the water rod; however,

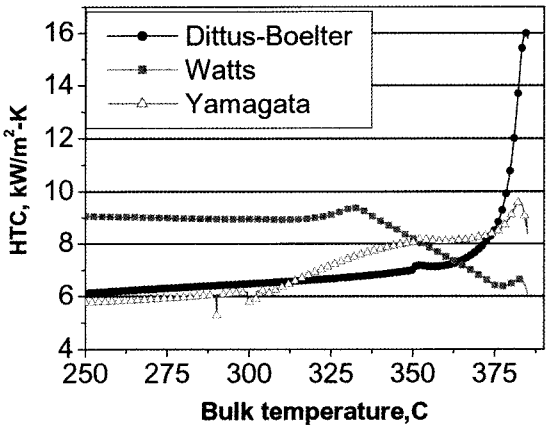

Fig. 13. Heat Transfer Coefficient (HTC) by Different Correlations for Water rod (P=25MPa, G=558kg/s·m², Q=500kW/m², D=0.036m)

the direction of heat transfer is changed in the lower part. In spite of a large variety of heat transfer correlations proposed in the literature, an adequate solution has yet to be achieved. On the other hand, heat transfer coefficient affects both the temperature distribution of the moderator and the power distribution. Fig. 13 presents the calculated heat transfer coefficient with different correlations under conditions typical of a SCWR water rod. More details about the effect of the heat transfer coefficient on the core power and other parameters can be found in reference [12].

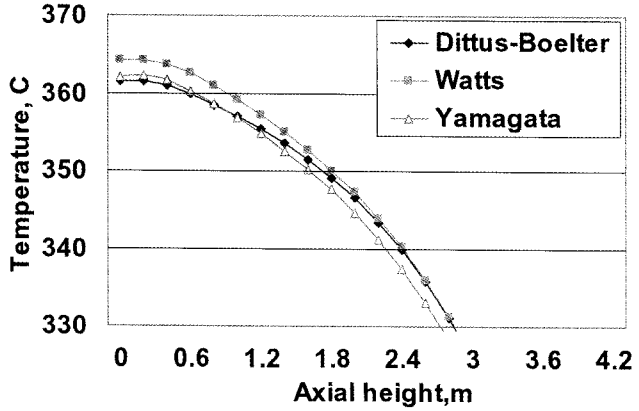

Fig. 14. Moderator Temperature with Different HTC Correlations for Water Rod

Fig.14 shows the average moderator temperature with different heat transfer correlations for the moderator channel. Due to larger HTC (see Fig.13), Watts correlation gives a higher moderator temperature. The moderator will affect the power and thermal hydraulic results (see Table 5). With a larger HTC between the water rod and fuel channels, the Watts correlation achieves not only a higher moderator temperature, lower hot channel factor, and lower hot spot factor, but also a higher maximum cladding temperature and a smaller K_{eff} value.

Table 6 shows some results according to different multiplication factors for the heat transfer coefficient calculated by the correlation given by Watts. In Table 6

Table 5. Comparison of Results Using Different Heat Transfer Correlations for Water Rod

Results	Dittus-Boelter	Watts	Yamagata
Nuclear hot channel factor (-)	1.072	1.070	1.077
2D (x-y) nuclear hot spot factor (-)	1.323	1.320	1.326
3D nuclear hot spot factor (-)	2.186	2.052	2.130
MCST (°C)	647.93	654.36	646.34
Max. fuel temperature (°C)	1688.42	1606.26	1660.76
Fuel channel inlet temperature (°C)	352.6	356.70	355.05
Max. moderator temperature (°C)	364.71	368.0	365.03
K_{eff}	1.089	1.089	1.091

Table 6. Comparison of Results between Different HTC Values for Water Rod

Results	Insulation	Normal	Enhanced
Nuclear hot channel factor (-)	1.063	1.070	1.071
2D (x-y) nuclear hot spot factor (-)	1.306	1.320	1.340
3D nuclear hot spot factor (-)	2.624	2.052	1.789
MCST (°C)	631.70	654.36	686.84
Max. fuel temperature (°C)	2017.53	1606.26	1420.26
Fuel channel inlet temperature (°C)	341.08	356.70	363.05
Max. moderator temperature (°C)	352.6	368.0	373.0
K_{eff}	1.099	1.089	1.084

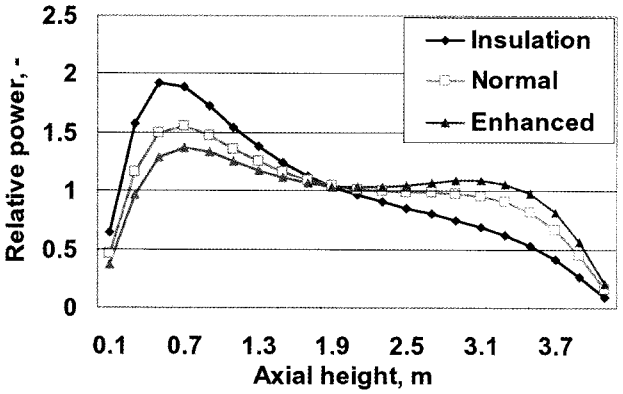

Fig. 15. Axial Power Distribution According to Different HTC Values (Only Related to Water Rod)

"Insulation" means a heat transfer multiplication factor of 1, "normal" a heat transfer multiplication factor of 2, and "enhanced" a heat transfer multiplication factor of 3. An increase in the non-uniformity of both the enthalpy rise and in the maximum cladding temperature is obtained with an increase in the HTC. This is due to strong variation in the axial power (see Fig.15) and a sharp increase in the fuel channel inlet coolant temperature. The HTC under insulation leads to a larger nuclear hot spot factor, a higher fuel central temperature, a lower moderator temperature, and, subsequently, a larger value of K_{eff}.

It should be pointed out that, with different multiplication factors for the heat transfer coefficient (HTC), there is a large change not only in the axial and radial power distribution but also in the maximum cladding temperature and the hot channel factor. Therefore, the heat transfer coefficient between the water rod and the fuel channel is of great importance for the SCWR core design.

7. SUB-CHANNEL ANALYSIS

In order to more accurately evaluate the local parameter distribution inside the fuel assemblies, a coupling analysis is carried out for the thermal-hydraulics in the sub-channel scale and neutron-physics in the pin-wise scale of the hottest fuel assembly. The FA averaged values of some parameters, such as power generation, mass flux and moderator flow rate, are taken from the previous coupling core calculation presented in chapter 5.

Based on the results from the core analysis, FA 3 is considered as the hot FA and is selected for further investigation with the sub-channel analysis. Due to the geometric symmetry, only one-fourth of the fuel assembly is taken into consideration. The numbering system for fuel rods and sub-channels is indicated in Fig. 16.

The coupling procedure is the same as the core analysis

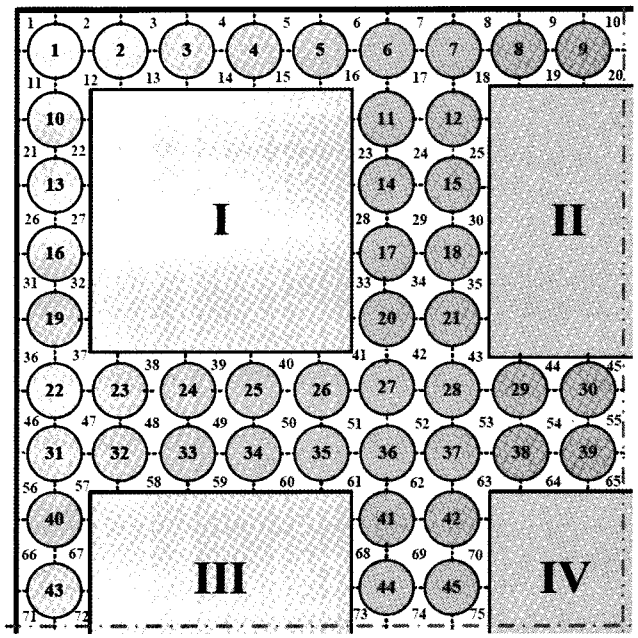

Fig. 16. Scheme of Sub-channel and Fuel Rod

in part 4. For the neutronic calculation, the total reflective boundary condition is applied to the radial boundary condition (BC), and the zero neutron flux is applied to the axial BC (extrapolated distance is 0.0 cm). It should be pointed out that the pin-wise power distribution in a fuel assembly could be influenced by the surrounding assemblies and the arrangement of the control rod and burnable poison, which will be taken into consideration in future work. For the thermal hydraulic analysis, the Bishop correlation [12] and the Rehme correlation [14] are selected for the evaluation of the cladding temperature and the friction factor. A turbulent mixing factor of 0.02 is applied to COBRA-IV to predict the mixing behaviour of the adjacent sub-channels.

Table 7 gives some calculated results of FA 3. The total heat generated in this 1/4 FA is about 2797.4 kW, the inlet coolant temperature is 356.70°C, and the bundle average coolant mass flux is 665.70 kg/m^2·s. The moderator mass flux is 447.42 kg/m^2·s, and the highest moderator temperature is 369.60°C, which occurs at the lower part of the moderator channel IV. For the radial power distribution, the maximum and minimum rod power factor is 1.092 and 0.838, respectively. The maximum power pin is the central fuel rod (fuel rod 45). The hottest channel is the central sub-channel (SC 52), with the hot channel factor being 1.139. This is due to the inner fuel rods receiving better moderation and releasing more power in this location, while at the same time SC 52 is not connected to the water rod. These two factors cause SC 52 to be the hottest channel, and the maximum coolant temperature

Table 7. Some Calculation Parameters and Results for Fuel Assembly #3

Parameters and Results	values
Total thermal power (kW)	2797.4
Coolant average mass flux (kg/m^2·s)	665.70
Coolant inlet temperature(°C)	356.70
Coolant outlet temperature(°C)	518.00
Max. coolant temperature (°C)	594.80
Moderator mass flux (kg/m^2·s)	447.42
Max. moderator temperature (°C)	369.60
x-y max.& min. power factor (-)	1.092/0.838
Nuclear hot channel factor (-)	1.139
Nuclear hot spot factor (-)	1.755
MCST (°C)	674.71
Max. fuel temperature (°C)	1269.53
K_∞	1.081

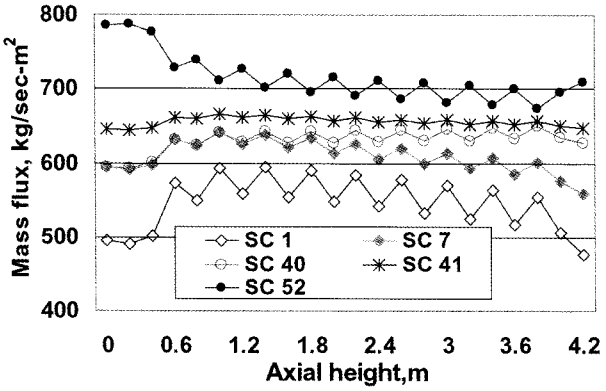

Fig. 17. Coolant Mass Flux in Various Sub-channels

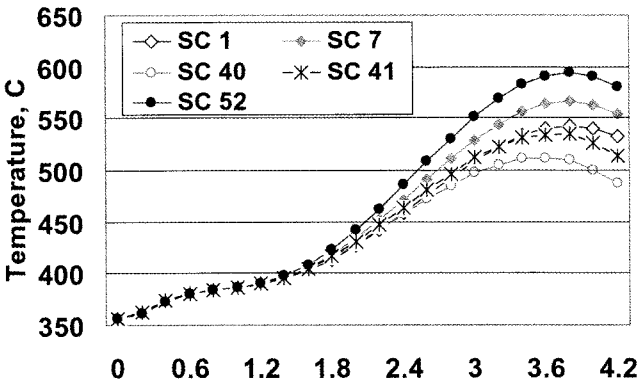

Fig. 18. Coolant Temperature Distribution in Various Sub-channels

also occurs here (594.80°C). Due to the maximum radial power pin of fuel rod 45, the nuclear hot spot factor is at the lower part of this rod, with a value of 1.755. This leads to occurrence of the maximum fuel temperature at this point (about 1269.53°C). The maximum cladding surface temperature (MCST) also takes place at the top of this fuel rod, with a value of 674.71°C.

It should be point out that the previous core design analysis shows that the maximum cladding temperature of FA 3 is about 654 °C (see Fig. 10). In this sub-channel calculation, the nominal peak cladding temperature is 674.71°C, which is about 20°C higher than that evaluated by the core analysis using homogenized coolant temperatures.

Fig.17 presents the coolant mass flux and temperature distribution in different sub-channels. Sub-channel 1 (SC 1) is located in the corner of the assembly and has the smallest hydraulic diameter (3.05mm) among all the sub-channels. The smallest hydraulic diameter leads to the lowest mass flux in SC 1 [7]. The coolant mass flux in SC 1 is about 20% lower than that in SC 52, the hydraulic diameter of which is 6.67mm. Note that the mass flux in SC 7 and SC40 shows satisfactory agreement in the bottom of the FA, and a large difference at the exit of the FA, although the hydraulic diameters of the two sub-channels are the same. This is due to the temperature distribution in the two channels. SC 7 has a higher coolant temperature, which results in lower density and lower mass flux in this channel.

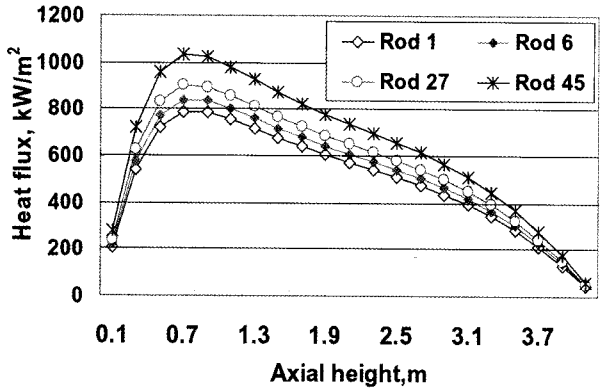

Fig. 19. Heat Flux of Various Fuel Rods

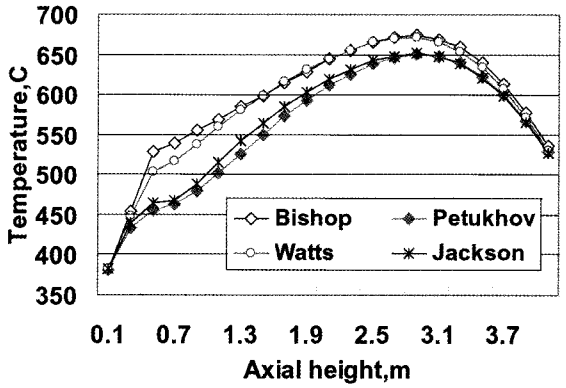

Fig. 21. Cladding Temperature Distribution of Fuel Rod 45

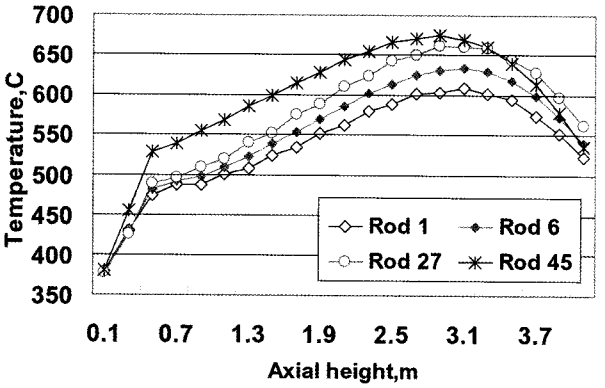

Fig. 20. Cladding Temperature of Various Fuel Rods

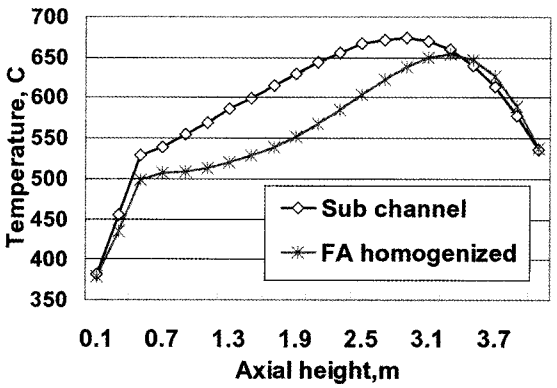

Fig. 22. Cladding Temperature Distribution of the FA Homogenized and Sub-channel Calculation

Fig. 18 shows the coolant temperature distribution in various sub-channels. Due to SC 40 and SC 41 being adjacent to the moderator channel, direct heat transfer occurs from the coolant to the moderator, and thus the temperature in these two sub-channels shows lower values. It should be noted that in the lower part of the FA, where the coolant temperature is below the pseudo-critical point, satisfactory agreement of the coolant temperature is obtained among different sub-channels. However, when the temperature is beyond the pseudo-critical point, a considerable difference is found among the various sub-channels. This could be caused by the low specific heat above the pseudo-critical point, leading to larger temperature differences at this location with different enthalpies. Further investigation should be performed to obtain better understanding of this phenomenon.

Fig. 19 shows the heat flux on various fuels rods. It is clear that with the fuel rod from the outer zone to the inner zone of the FA, there is an increase of the fuel rod surface heat flux. This is due to better moderation for the inner fuel rods. The axial power peak locates at the lower part of the FA, since there is high water density here. Fig. 20 shows the cladding temperature distribution of the various fuel rods. The central fuel rod 45 shows the highest cladding temperature due to the greater power generation of this rod. As shown in Fig. 20, the cladding temperature of fuel rod 27 is as high as that of fuel rod 45. This is due to the hot channel (SC 52) being next to fuel rod 27. Therefore, the large value of coolant enthalpy in SC 52 leads to a high cladding temperature.

Fig. 21 presents the calculated cladding temperature profile of fuel rod 45 using different heat transfer correlations [12]. The results indicate that the Bishop and Watts correlations give a higher maximum cladding temperature, which locates in the upper part of the active height. The other two correlations give a maximum cladding temperature below the upper design limit of 650°C, which approaches the outlet of the FA. The Bishop and Watts correlations also predict a higher cladding temperature

peak in the lower part of the fuel assembly, which corresponds to the high heat flux at this location.

Fig. 22 shows the cladding temperature of fuel rod 45 calculated by different analysis methods: the sub-channel and FA homogenized analysis. The results indicate the sub-channel analysis gives a 20°C higher maximum cladding temperature than the FA homogenized method.

8. CONCLUSION AND FUTURE WORK

A SCWR thermal core using PWR-type two-row fuel assemblies is proposed. The total core thermal power is 3500 MW, and the average linear power density is 19kW/m. The inlet and outlet coolant temperature is 280°C and 508°C, respectively. The fissile assemblies have 3 different enrichments in order to flatten the radial power profile. The coolant and moderator mass flow in different fuel assemblies are specified to achieve quasi-optimized thermal-hydraulic behavior and a uniform power distribution.

The thermal hydraulic results indicate that the maximum cladding surface temperature and the maximum fuel temperature are 654°C and 1606°C, respectively. The neutronic calculation presents that the core arrangement with different enrichments gives a negative temperature reactivity coefficient. The maximum linear heat generation rate over the core is 38.9kW/m. Therefore, some important design criteria are satisfied well for the reactor core with the given reference parameters.

A strong effect of the heat transfer correlation on the maximum cladding temperature and power distribution is identified. For the fuel channel, the correlations of Swenson and of Bishop give the highest cladding temperature, whereas the Dittus-Boelter correlation gives the lowest temperature. The difference in cladding temperature predicted by various correlations is as high as 50°C. From the point of view of safety, the correlations of Swenson and of Bishop are recommended for evaluation of the cladding temperature. Furthermore, the results indicate that special attention must be paid both to the power peak in the lower part of the core due to heat transfer deterioration phenomena and to the power peak in the upper part due to small specific heat and, subsequently, small heat transfer coefficients. In addition, the importance of the heat transfer between the water rod and the fuel channel is identified. This can cause a strong shift of the nuclear hot spot factor from 1.789 to 2.624, when the heat transfer coefficient is changed by a factor of 3. This would result in a strong increase in the fuel temperature.

Based on the sub-channel analysis of the hottest fuel assemblies, a strong heterogeneity of the sub-channels and fuel rods within this assembly is identified. The mass flux in SC 52 is about 15% higher than that in SC1. Fuel rod 45 shows the highest cladding temperature, with a value 674.7°C, about 20°C higher than the value obtained with the FA homogenized analysis approach. The results clearly indicate the importance of the sub-channel analysis, which can more accurately provide the local parameter distribution inside the fuel assemblies.

Further investigations on this thermal SCWR core design are ongoing. A detailed analysis of the burn-up performance will be carried out with the coupled neutron-physical/thermal hydraulic approach. The parameters with burn-up and the excess reactivity control methods will be considered in future work. If necessary, modification and improvement of both the fuel assembly and core structure will be made.

ACKNOWLEDGMENTS

The authors would like to thank the National Basic Research Program of China (No.2007CB209804) for providing financial support for this study.

REFERENCES

[1] Y. Oka, "Review of High Temperature Water and Steam Cooled Reactor Concepts", *Proc. of SCR-2000,* Tokyo, Japan, Nov.6-8, 2000.

[2] A. Yamaji, K. Kamei, Y. Oka, et al, "Improved Core Design of the High Temperature Supercritical-Pressure Light Water Reactor", *Annals of Nuclear Energy*, **32**, 651 (2005).

[3] K. Kamei, A. Yamaji, Y. Ishiwatari, "Fuel and Core Design of Super LWR with Stainless Steel Cladding", *Proceedings of 2005 International Congress on Advances in Nuclear Power Plants (ICAPP '05)*, Seoul, Korea, May 15-19, 2005.

[4] T. Schulenberg, J. Starflinger, J. Heinecke, "Three Pass Core Design Proposal for a High Performance Light Water Reactor", *Progress in Nuclear Energy*, **50**, 526(2008).

[5] T. Schulenberg, and J. Starflinger, "European Research Project on High Performance Light Water Reactors", *3rd Int. Symposium on Supercritical Water-Cooled Reactors-Design and Technology*, Shanghai, China, March 12-15, 2007.

[6] X.J. Liu, X. Cheng, "Thermal-hydraulic and Neutron-physical and Characteristics of a New SCWR Fuel Assembly", *Annals of Nuclear Energy*, **36**, 28 (2009).

[7] X. Cheng, T. Schulenberg, D. Bittermann, P. Rau, "Design Analysis of Core Assemblies for Supercritical Pressure Conditions", *Nuclear Engineering and Design*, **223(3)**, 279 (2003).

[8] C. Waata, T. Schulenberg, X. Cheng, "Results of a Coupled Neutronics and thermal-hydraulics Analysis of a HPLWR Fuel Assembly", *Proceedings of 2005 International Congress on Advances in Nuclear Power Plants (ICAPP '05)*, Seoul, Korea, May 15-19, 2005.

[9] A. Yamaji, T. Tanabe, Y. Oka, et al, "Evaluation of the Nominal Peak Cladding Surface Temperature of the Super LWR with Sub-channel Analyses", *Proceedings of GLOBAL 2005*, Tsukuba, Japan, Oct 9-13, 2005.

[10] X.J. Liu, X. Cheng, "Coupling Analysis on a New SCWR Core Design", *Proceedings of 2008 International Congress on Advances in Nuclear Power Plants (ICAPP '08)*, Anaheim, CA USA, June 8-12, 2008.

[11] P. E. MacDonald, J. Buongiorno, J.W. Sterbentz, et al, "Feasibility Study of Supercritical Light Water Cooled Reactors for Electric Power Production", *INEEL/EXT-04-*

02530, Idaho National Engineering and Environmental Laboratory (2005).
[12] X. Cheng, T. Schulenberg, "Heat Transfer at Supercritical Pressures-Literature Review and Application to an HPLWR", *FZKA 6609*, Forschungszentrum Karlsruhe, (2001).
[13] M. J. Watts and C. T. Chou, "Mixed Convection Heat Transfer to Supercritical Pressure Water", *Proceedings of 7th Int. Heat Transfer Conf.*, Munich, Germany, Sep. 6-12, 1982.
[14] K. Rehme, "The Structure of Turbulence in Rod Bundles and the Implications on Natural Mixing between the Subchannels," *Int. Journal of Heat and Mass Transfer*, **35**, 567 (1992).